APPLICATION OF JOINT RECEIVER-FUNCTION SURFACE-WAVE DISPERSION FOR LOCAL STRUCTURE IN EURASIA

Robert B. Herrmann, Charles. J. Ammon, and Jordi Julia
Saint Louis University

Sponsored by Defense Threat Reduction Agency

Contract No. DTRA01-00-C-0214

ABSTRACT

Subsurface geology generally has a broad wave number spectrum containing sharp, or high wave-number, changes in velocity near major geologic boundaries and smooth low wave-number variations in regions of relatively uniform geologic structure. Access to the full spectrum of earth structure requires that we exploit signals that span a wide frequency range and that are sensitive to the entire spectrum of heterogeneity. Our research is targeted at improving resolution of the full range of earth heterogeneity by combining seismic data sets traditionally analyzed separately. We will present the results of our efforts to combine teleseismic P-wave receiver functions and surface-wave dispersion measurements in a joint inversion for the variation in shear-wave velocity with depth in the lithosphere. Receiver functions are primarily sensitive to shear-wave velocity contrasts and vertical travel times, whereas surface-wave dispersion measurements are sensitive to vertical shear-wave velocity averages. Their combination bridges resolution gaps associated with each individual data set. The data are inverted using a joint, linearized inversion scheme which accounts for the relative influence of each set of observations, and allows a trade-off between fitting the observations, constructing a smooth model, and matching *a priori* constraints. Receiver functions are readily calculated using P-waveforms from distant earthquakes, and waves arriving from different directions can provide information on lateral variations in earth structure. Intermediate- to long-period dispersion values are available from global and regional tomographic studies and can be supplemented at the shortest periods using direct measurements from recordings from nearby events (when they are available). We will illustrate our work using applications to station TAM in North Africa and Eurasia (several portable stations in Tibet, station KIV, NIL, ABKT, BRVK, KURK, and WUS). Naturally, the inversion results depend on the quality of the data, and we are also investigating the changes in earth structure parameters that result from using dispersion values from different tomographic studies. To test the estimated earth models, we compare high-frequency regional-distance synthetic seismograms and regional earthquake waveforms.

KEY WORDS: earth models, shear-velocity, surface-wave dispersion, receiver functions

OBJECTIVES

Although epicentral location can be a clear discriminant in many cases, instances in which waveform measures such as accurate event depth or $M_S \backslash m_b$ ratios will be needed to help resolve ambiguity remaining after accurate event location. To study small seismic events, we must produce models that are useful for isolating and enhancing small-event seismic signals, which generally have small amplitudes and are noisy (Figure 1). The better we can enhance these marginal signals, the better we can estimate parameters such as event size, location, and depth. Our research is directed towards developing and applying methods for refining shear-velocity earth models to the point where they can contribute to mode isolation and enhancement, particularly at short periods where surface-wave tomography results can be extrapolated, but are limited by sparse data availability. Such models may also help with the most difficult event location parameter, depth. We have adopted the philosophy that advances in lithospheric structure modeling require the simultaneous fitting of complementary data to constrain the entire wave number spectrum of seismic velocity variations. In addition, *a priori* information on geologic structures, thermal environment, and tectonic history will likely be needed to construct the reliable estimates of subsurface geology. Our focus in this contract has been to test

and to exercise the joint inversion of receiver function and surface-wave dispersion (e.g. Julia et al., 2000) by comparing earth model estimates with those developed independently and by investigating the use of these models for seismogram modeling.

Combining Seismic Data in Composite Inversions

Subsurface geology generally has a broad wave-number spectrum, containing sharp, or high wave-number, changes in velocity near Earth s surface, at the sediment-basement transition, near the crust-mantle boundary (usually), and in the upper-mantle transition zone, and smooth low wave-number variations in regions of relatively uniform geologic structure. Access to the full spectrum of earth structure requires that we exploit signals that span a wide frequency range and that are sensitive to the entire spectrum of heterogeneity. For example, surface-waves, travel times, and direct-wave amplitudes are sensitive to smooth variations in earth structure; reflected and converted waves are sensitive to the velocity contrasts.

Joint inversions is an obvious approach to improve estimates of earth structure. Refraction seismologists have long used seismic wave travel times, amplitudes, and gravity variations to study the structure along one-dimensional surface profiles that illuminate the two-dimensional subsurface geology. To successfully combine data in an inversion, we must insure that all the data are sensitive to the same (or related) physical quantities and that they sample or average structure over comparable length scales. Recent advances in surface-wave tomography have provided an opportunity to combine localized surface-wave dispersion estimates with other data such as P- and S-wave receiver functions.

Surface-wave dispersion measurements are sensitive to broad averages, or long wave-number components of earth structure (e.g. Brune, 1969; Der et al., 1970; Braile and Keller, 1975, Ozalaybey, et al., 1997). They provide valuable information on the absolute seismic shear velocity but are relatively insensitive to sharp (high wave-number) velocity changes. Generally surface-wave inversions must be constrained using a particular layer parameterization (e.g. near-surface, upper-crust, lower crust, mantle lid, deep mantle), must resemble an *a prior* model, or must be substantially smoothed to stabilize earth-structure estimation Receiver functions are time series, computed from three-component body-wave seismograms, which show

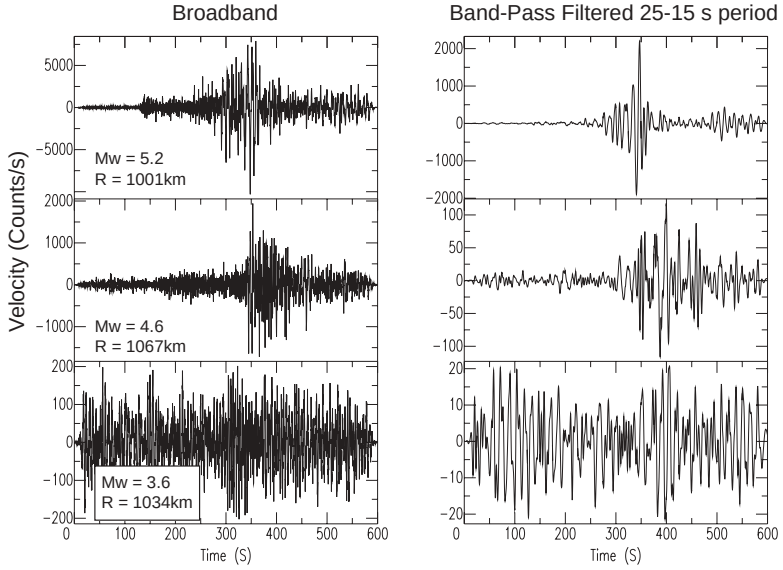

Figure 1. Illustration of the variation of signal frequency content for a source-receiver distance of about 1000 *km*. The signals on the left were generated by earthquakes in the Tien Shan region and recorded at station WMQ in central Asia. Those on the right are band-pass filtered version of the raw signals with a filter passing periods between 25 and 15 second (spanning the 20s Ms measurement range). The surface wave of the *Mw* 3.6 event is visible in the noisy trace at the bottom. Enhancing the signal to make an Ms measurement would require an appropriate short-period phase-match filter. *Mw* values are from moment-tensor inversion (Ghose et al., 1998).

the relative response of Earth structure near the receiver. Source effects are removed from the seismograms using a deconvolution that sacrifices P-wave information for isolation of near-receiver effects. Receiver function waveforms are a composite of P-to-S (or S-to-P) converted waves that reverberate within the structure beneath the seismometer (e.g. Langston, 1979; Ammon et al., 1990; Ozalaybey, et al., 1997). Modeling the amplitude and timing of those reverberating waves can supply valuable constraints on the underlying geology. In general, the receiver functions sample the structure over a range of 10 s of kilometers (roughly the one -to-two times the depth of the deepest interface) from the station in the direction of wave approach. Stations sited near geologic boundaries can produce different responses for different directions.

RESEARCH ACCOMPLISHED

Improved Receiver Function Estimation Procedure

When the data are high-quality and the receiver structure is not too complex, the choice of a deconvolution procedure used to estimate receiver functions does not make much difference. However, when the noise in the seismograms is substantial, or the receiver structure is complex, different deconvolution approaches have strengths and weaknesses. We compute receiver functions using the iterative time-domain deconvolution procedure described by Ligorria and Ammon (1999). We prefer the iterative approach, which is based on the Kikuchi and Kanamori (1982) source-time function estimation algorithm, for several reasons. First, in the iterative approach the receiver function is constructed by a sum of Gaussian pulses which produces a flat spectrum at the longest periods. The flat long-period spectrum can be viewed as *a priori* information that helps reduce side-lobes that may result of spectral or singular-value truncation stabilization procedures. The reduction of side-lobes eases the interpretation and helps stabilize low-frequency receiver functions. Second, the iterative approach constructs a causal receiver function, which is what we expect in all cases of reasonable earth structure. This is a subtle difference from spectral techniques [*e.g. Langston, 1979; Park, 2000*] which can always introduce a component to the receiver before the P-wave. The acausal component of the spectral signal may be small, but still important to the satisfaction of the convolutional model that defines a receiver function, *i.e.:*

$$R(t) = Z(t) * E_R(t) . \quad (1)$$

In equation (1), $R(t)$ and $Z(t)$ are the radial and vertical seismograms, and $E_R(t)$ is the radial receiver function (a similar equation holds for the transverse component). The point is that even when the receiver function estimation is unstable, spectral deconvolutions may satisfy (1) quite well. The iterative time-domain approach, which can be restricted to produce the best *causal* solution, may not always satisfy (1). Experienced modelers have always been able to identify failed receiver functions, but the misfit to (1), available from iterative deconvolutions, provides quantitative information that can be be used to quantify deconvolution reliability, and thus used when stacking signals, or in extreme cases, to discard obviously failed deconvolutions.

An Illustration of the Joint Inversion: Station ABKT, Alibek, Turkmenistan

At the Research Review, we will present results from several stations throughout North Africa and western Asia. Here we illustrate the joint inversion procedure using a single example from central Asia, station ABKT, Alibek, Turkmenistan (Figure 2). ABKT is located along a northwest-southeast striking boundary between the Iranian Plateau and the Russian Platform (Figure 2). Southwest of the station lies the Iranian Plateau, a region elevated as a result of continental collision and part of the high-elevation plateaus that stretch from southern Europe to eastern Asia. North and east of ABKT is the southern Russian Platform, or specifically, the KoPet-Dag foreland. ABKT is situated within the thrust belt formed by the overthrusting of the Iranian Plateau onto the Russian Platform. Recent motion is not pure reverse, most of the larger, recent nearby focal mechanisms suggest right-lateral movement along structures parallel to the boundary (or left-lateral motion perpendicular to the boundary) (Figure 2).

To estimate the structure in the vicinity of ABKT, we used Stevens *et al.s* (2001) Rayleigh-wave dispersion estimates and receiver functions sampling the structure to the east of the station, towards the southern Russian Platform. ABKT is well situated for receiver function analysis because of a large number of teleseismic

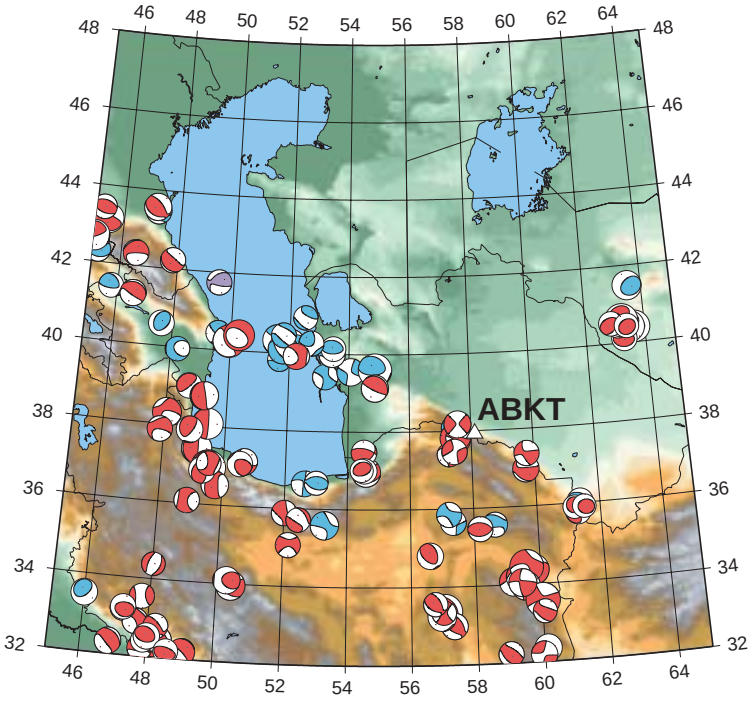

Figure 2. Location of station ABKTat Alibek, Turkmenistan (37.9304N, 58.1189E, 678 m), shown with topographic variations and focal mechanisms from the Harvard CMT catalog. Mechanisms are shaded by depth (red indicated depths from 0 to 32 *km*; blue depths from 33 to 70 *km*; and purple depths greater than 70 *km*).

events in the western Pacific subduction zones. The teleseismic P-waveforms are unevenly distributed with back azimuth (Figure 3), with a superb concentration to the east-northeast, but few signals arrive from the west-southwest. The number of events archived at the IRIS data management center decreases through the years 1995-1999. Although the data are sparse to the west, the sampling to the east will allow an analysis of variations in response to changes in incidence angle and eastern azimuths. The panel on the left shows few details in the receiver functions but clearly illustrates the available data distribution. The expanded view on the right of receiver functions sampling the structure from the northeast to southeast of ABKT illustrates strong coherence of many arrivals and some systematic changes. Arrivals approaching from the northeast contain two distinct arrivals at about 4.5 and 7.4 seconds, and a less coherent multiple arrives at about 13 seconds. The initial peak amplitude is shifted about 0.8 seconds late for northeast arriving waves and 0.2 seconds for southeast arriving waves. The shift is indicative of a large *Ps* conversion from the base of a sedimentary basin, which is expected to be more prominent at this site for waves coming in from the northeast.

We present results that correspond to the structure east of ABKT, computed using a subset of radial receiver functions using P-waves approaching from the east with relatively shallow incidence angles (ray parameters > 0.07 *s/km*) (Figure 4). For surface wave dispersion we use the Rayleigh wave dispersion curve from the model of Stevens *et al.* (2001), which is part measured and part extrapolated using *a priori* information. Dispersion values are very low at the short periods (Figure 4), indicative of a thick sequence of sediments. The deep mantle structure is constrained to merge with PREM to insure consistent results with global models. The inversion results are summarized in (Figure 4). The estimated shear-velocity model is fairly simple, with one unusual high-velocity layer near the crust-mantle boundary that was probably introduced to fit a trough in the receiver function. The fit to the dispersion is superb with the exception of the shortest periods. The model contains a 10- to 12-km sequence of low shear-velocity material that is likely the sediments of the KoPet-Dag foreland. Crustal thickness is about 42 km, although the transitional crust mantle boundary makes a precise thickness estimate difficult. The model agrees reasonably well with a structure near

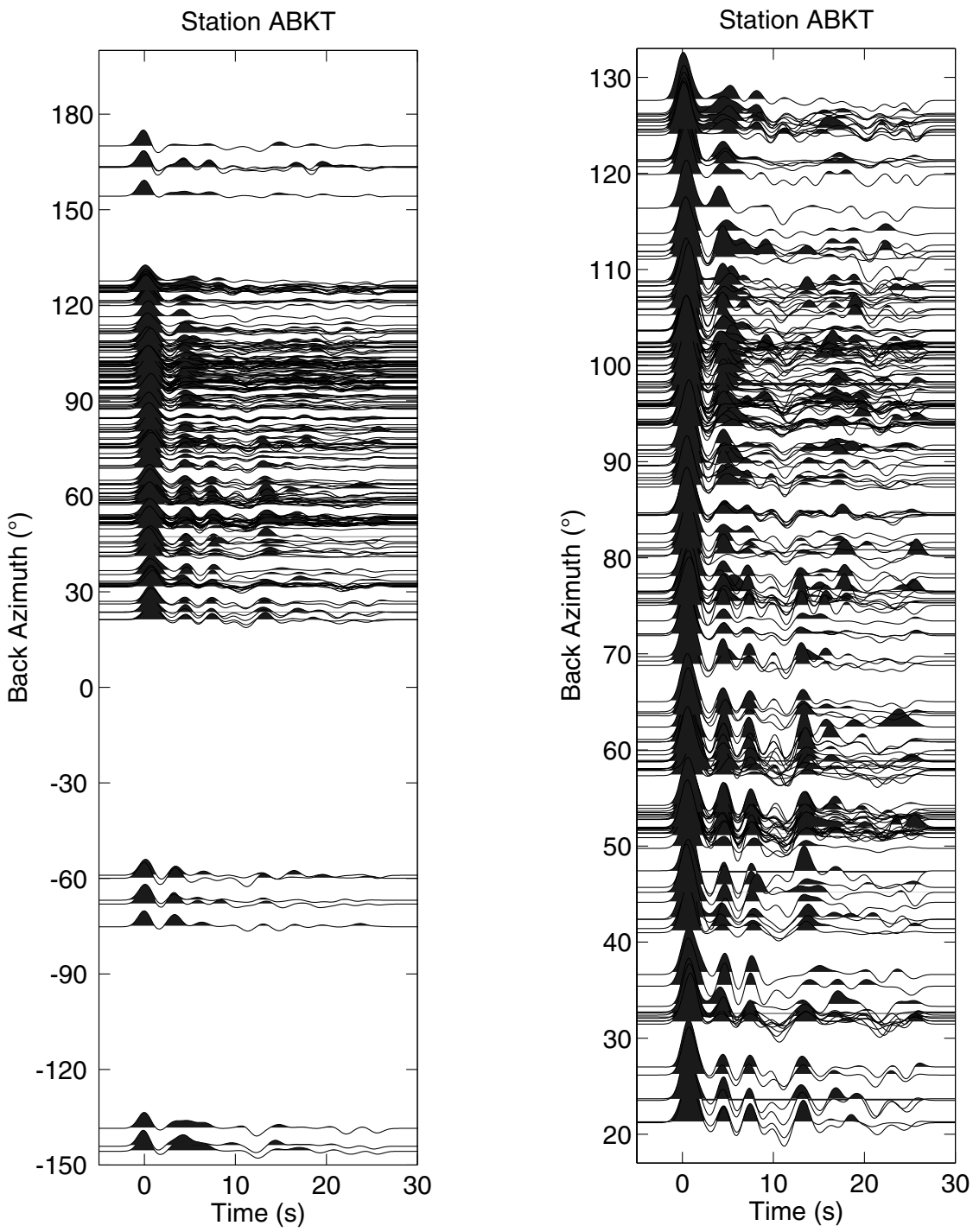

Figure 3. Receiver function estimates that meet a prediction misfit criteria of less than 10% of the power in the P-waveform. The full set of data are shown on the left, the panel on the right is an expanded version of the waveforms approaching the station with back azimuths between 20¡ and 130¡. Positive polarities are shaded. The data distribution is strongly biased tow the east-northeast, where ample data from the subduction zones provide a near continuous azimuthal distribution. Sparse data from the western azimuths makes imaging the Iranian Plateau structure more difficult (always a risk with stations near large geologic boundaries).

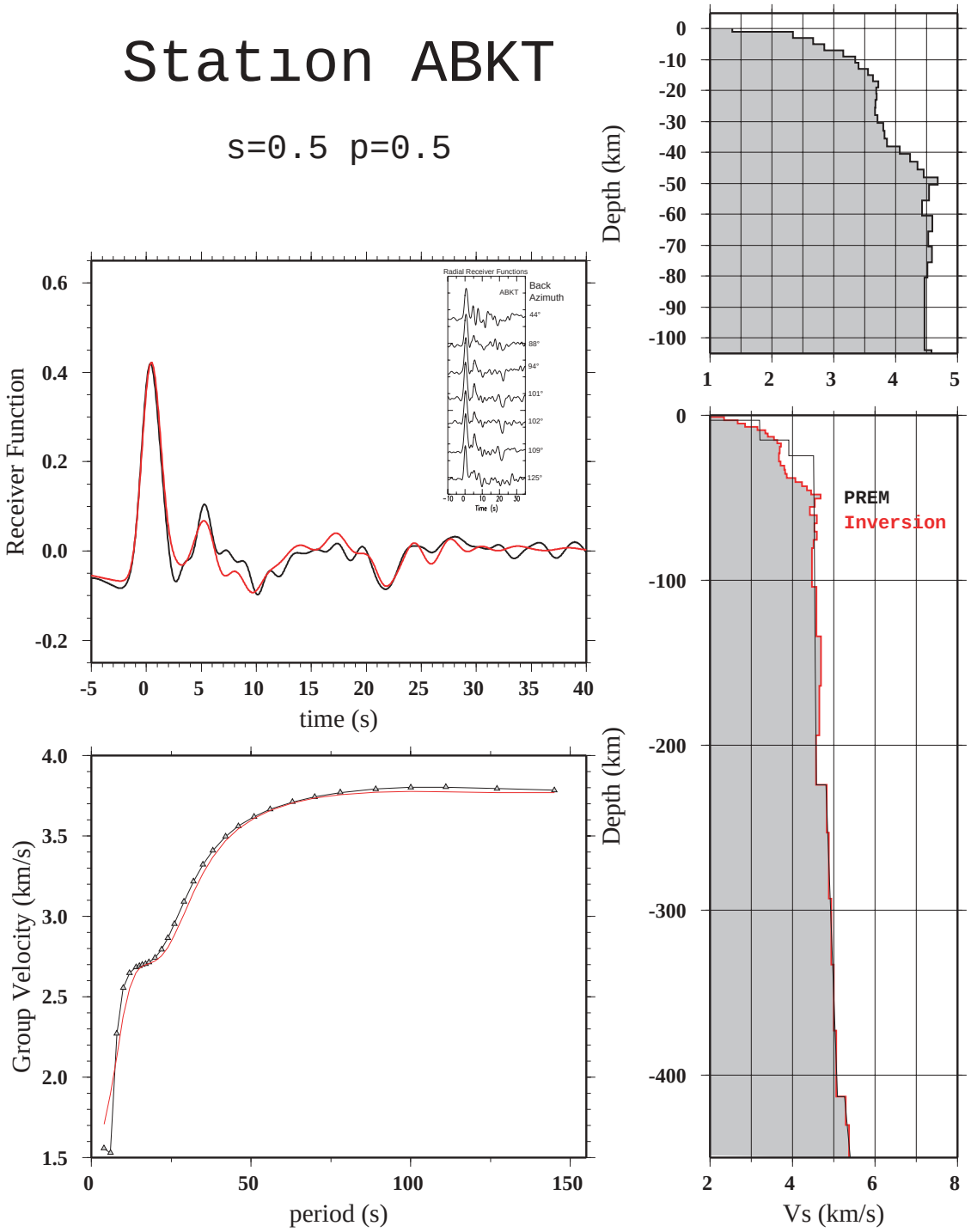

Figure 4. Inversion results for station ABKT using Stevens dispersion model and a receiver function appropriate for the region east-northeast of the station. Red lines identify predictions, black lines (and symbols) the observations. The subset of receiver functions used to compute the stack used in the inversion is shown in the inset of the upper left panel. The gray shaded models is the result of the inversion.

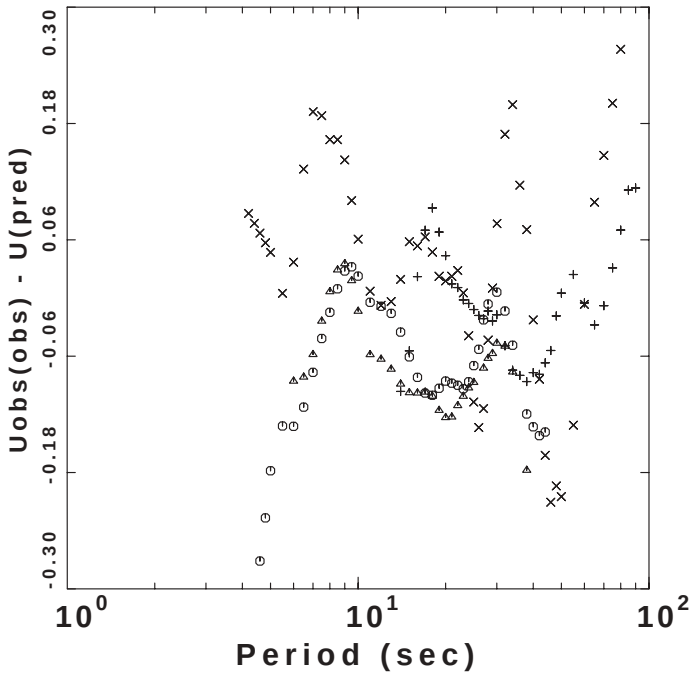

Figure 5. Difference between observed and predicted group velocity dispersion along 4 paths to the INCN station.

37.32¡N, 60.60¡E, listed in Christensen s article in the CRC Practical Handbook of Physical Properties of Rocks and Minerals (The original reference to work on Russian Platform in central Asia by Godin et al., 1961).

Dispersion Measurements

The surface-wave dispersion near the seismograph station is the least known quantity. One can use existing regionalizations (Stevens, Harvard, Colorado) or derive local dispersion. The Stevens technique provides Rayleigh-wave group velocity dispersion curves in the 4 - to 400-second-period range, uses a 1 x 1 degree global grid, is rooted in a global crustal model, and is constrained by observations in the 10 - to 100-second-period range. The Harvard regionalization provides phase velocity dispersion at longer periods.

We have tested the Stevens predictions in two different regions: northeast China platform near Korea and the central U. S. To study wave propagation near Korea, waveform data from the Inchon station were used. Figure 5 presents the difference between the observed Rayleigh-wave group velocity and that predicted between the epicenter and the Inchon station. The distances ranged from 450 to 1120 km. The Stevens predictions are good in the 10- to 100-second period range, but a similar comparison in the central U. S. shows that the Stevens predictions at shorter periods are not adequate over short paths because the shallow shear-wave velocities underlying his predictions are not correct and because shallow geology changes significantly over distances of 100 km.

We are working with researchers and students at Seoul National University to apply the joint-inversion method at 11 stations of the current KMA broadband network in the southern Korean peninsula. Previous work on receiver functions (Yoo, 2001) indicates the presence of a simple crust which can be modeled as a single layer over a half-space with a 32 km-thickness. We are acquiring waveform data from the KMA network to determine the receiver functions and also to estimate phase velocities. We are evaluating several phase velocity estimation techniques: interstation cross-correlation and p-tau stacking (McMechan and Yedlin, 1981). The p-tau stacking technique works surprisingly well. Figure 5 shows the locations of the KMA

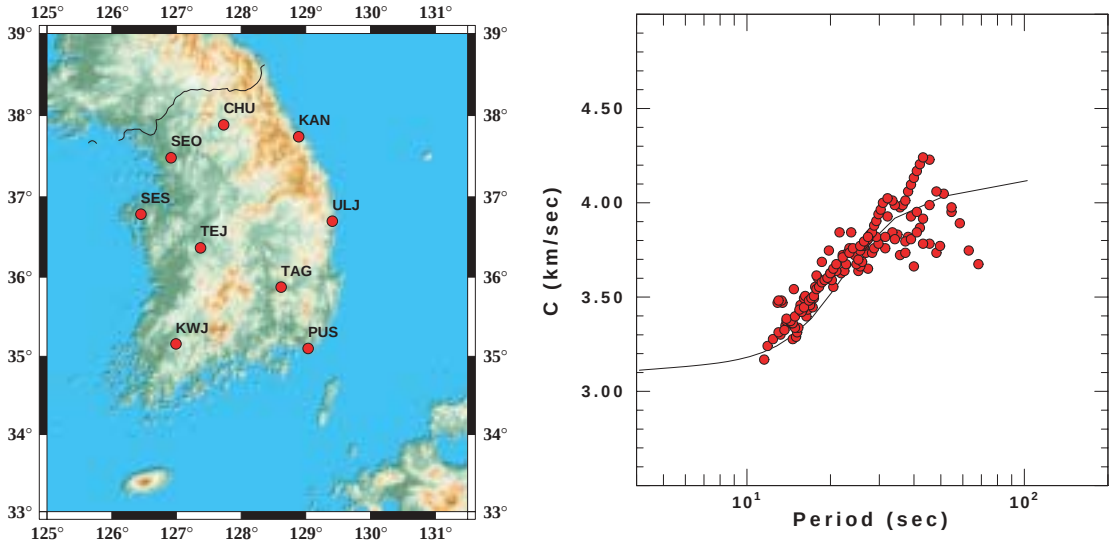

Figure 6. (Left) Location of 9 KMA stations used for phase velocity analysis. (Right) Comparison of theoretical fundamental mode Rayleigh-wave phase velocity dispersion for a simple velocity model for Korea and the p-tau processing results for three events at distances of 500, 2500 and 4000 km from Korea.

stations used a comparison of the derived phase velocity and a model prediction. The stability of the p-tau technique for both Love and Rayleigh waves is encouraging.

CONCLUSIONS AND RECOMMENDATIONS

The combination of receiver functions and surface waves produces robust earth models when the data are high quality. Our analysis generally shows that the models are consistent with other subsurface imaging results. To reliably constrain shear velocities in the upper crust, short-period 5- to 15-s surface waves are needed. Variations in earth structure estimates can be traced back to variations in surface-wave tomographic reconstructions. Additional tomographic work and direct comparisons of various models are needed to help better resolve uncertainties in the dispersion curves available for joint inversions. The Stevens group velocity prediction tool is very useful in regions for which no dispersion observations are available. It would be very useful if the Stevens tool could also predict Love-wave dispersion. Dispersion data for periods less than 10 sec must be acquired in order to properly constrain the upper crustal structure. The joint inversion technique succeeds in defining a local crustal structure for modeling intermediate- to long-period waveforms.

REFERENCES

Ammon, C.J., G.E. Randall, and G. Zandt (1990). On the non-uniqueness of receiver function inversions, J. Geophys. Res., 95, 15303-15318.

Braile, L., and G.R. Keller (1975). Fine structure of the crust inferred from linear inversion of Rayleigh-wave dispersion, Bull. Seism. Soc. A., 65, 71-83.

Brune, J.N. (1969). Surface waves and crustal structure, in The Earth's Crust and Upper Mantle, edited by P.J. Hart, pp. 230-242, American Geophysical Union, Washington, D.C.

Der, Z., R. Masse, and M. Landisman (1970). Effects of observational errors on the resolution of surface waves at intermediate distances, J. Geophys. Res., 75, 3399-3409.

Juli , J., C.J. Ammon, R.B. Herrmann, and A.M. Correig (2000). Joint inversion of receiver function and surface wave dispersion observations, Geophys. J. Int., 143, 1-19.

Kikuchi, M., and H. Kanamori (1982). Inversion of complex body waves, Bull. Seism. Soc. Am., 72, 491-506.

Langston, C.A. (1970). Structure under Mount Rainier, Washington, inferred from teleseismic body waves, J. Geophys. Res., 84, 4749-4762, 1979.

Ligorria, J.P., and C.J. Ammon (1999). Iterative deconvolution of teleseismic seismograms and receiver function estimation, Bull. Seism. Soc. Am., 89, 1395-1400.

McMechan, G. A. and M. J. Yedlin (1981). Analysis of dispersive waves by wave field transformation, Geophysics 46, 869-874.

Ozalaybey, S., M.K. Savage, A.F. Sheehan, J.N. Louie, and J.N. Brune (1997). Shear-wave velocity structure in the northern Basin and Range Province from the combined analysis of receiver functions and surface waves, Bulletin of the Seismological Society of America, 87 (1), 183-199.

Park, J., and V. Levin (2000). Receiver functions from multiple-taper spectral correlation estimates, Bulletin of the Seismological Society of America, 90 (6), 1507-1520.

Stevens, J. L. (2001). Global Rayleigh Wave Dispersion Atricle, Pure and Applied Geophys., in press.

Yoo, Hyun-Jae (2001). Crustal structure under the TJN station by receiver function methods, M. S. Thesis, Seoul National University, 56pp.